

Modeling and Performance Analysis of Planar Parallel Manipulators

Amr Abo Salem^(✉), Tarek Y. Khedr, Gamal El Ghazaly, and M.I. Mahmoud

Department of Industrial Electronics and Control Engineering,
Faculty of Electronic Engineering at Menouf, Menofia University, Menouf, Egypt
eng.amr.abo.salem@gmail.com, tarekyk04@yahoo.com, gamal.elghazaly@lirmm.fr,
m.i.mahmoud@yahoo.com

Abstract. Recently, the Parallel Manipulators (PMs) attract the attention of the researchers. This research work is concerned with the Planar Parallel Manipulators (PPMs). An investigation led to a comparative study between the 2-RRR PPM and 3-RRR PPM. The 2-RRR non redundant PPM and 3-RRR redundant PPM, with 2-degree-of-freedom, are considered. These two PPMs are introduced with their mechanism construction. The workspace, different properties and performance indices are carried out. Investigation of characteristics of these manipulators should go through the complexity of the direct and inverse kinematics problems, which are solved using the suggested and proper geometrical equations. The dexterous workspace is geometrically obtained where the End-Effector (EE) can reach and illustrate some of its properties. The Jacobian matrix for these manipulators is essential method to complete this analysis. This work is terminated by two characteristic maps of these two manipulators, which are dexterity and manipulability indices that were covering the workspace.

Keywords: Planar Parallel Manipulator (PPM) · End-Effector (EE) · Redundant and non-redundant · Direct Geometric Model (DGM) · Inverse Geometric Model (IGM) · Degree of Freedom (DOF) · Workspace · Jacobians matrix · Dexterity Index (DI) · Manipulability index (MI)

1 Introduction

Parallel Manipulator (PM) can be defined as a closed loop mechanism composed of an end-effector (EE) and a fixed base linked together by at least two independent kinematic chains. A serial manipulator referred as an open-loop manipulator because its one end connected to ground and other end is free to move in space. Significance of parallel manipulator over serial manipulator is its higher payload-to-weight ratio, high accuracy, high structural rigidity and low inertia of moving parts. Because the external loads can be shared by the actuators, parallel manipulators tend to have a large load-carrying capacity. On the other hand,

they suffer from relatively small workspaces, complex kinematics and highly singular workspaces. It is considered that PM have a great importance in many industrial and medical applications rather than in flight simulations [1]. This importance came from its design such as the length of the links, types of the joints, position of the actuators, the workspace, velocity and acceleration of the end-effector, ... etc. There are a lot of approaches applied to the PM, that lead to a good performance [2–4]. According to the types of joints, which are Revolute (R) and Prismatic (P), there are seven different types of configuration for a single arm which can be classified as *RPP*, *RRP*, *RRR*, *RPR*, *PRR*, *PRP* and *PPR* and they are reported in [5]. These configurations produce a lot of PPM such as 3-RRR. Researchers have focused their works for spatial parallel manipulators but usage of such planar configurations may not be neglected. The majority of studies on PM [6, 7], unlike serial manipulators, however, the redundancy can be divided into *actuation redundancy* and *kinematic redundancy*. *Actuation redundancy* can be explained as replacing existing passive joints of a manipulator by active ones. Consequently, actuation redundancy does not change the mobility or force workspace of a manipulator but may cause singularity reduction [8]. *Kinematic redundancy* occurs when extra active joints and links are added to manipulators. Adding kinematic redundancy in parallel manipulators have many advantages such as avoiding most kinematic singularities, enlarging workspace, and also improving dexterity [9]. However, when a manipulator is kinematically redundant, the complexity of actuation schemes is greater since there is an infinite number of solutions for the inverse displacement problem, and therefore, an infinite choice of actuation schemes. There are many research that consider the control of redundant and non-redundant PM [11–16]. To study these types of manipulators, it is essential to fully investigate and analyze the inverse displacement and the workspace. PMs can give both multiple inverse kinematic solutions and multiple direct kinematic solutions. Various applications of such 3-RRR planar parallel configurations are pick and place operation over a plane surface, machining of plane surfaces and mobile base for a spatial manipulator. The main subject of this work is the comparison of 5-bar mechanism which can be written as 2-RRR PPM and three arm PPM which can be written as 3-RRR PPM. Understanding the operation of the PPM needs to have a deep theoretical background and simulation of the robots as it will be explained as the next explanation.

2 Parallel Manipulator's Structure

2.1 Review

Going through the mechanics motion of the closed loop mechanism, it is found that the 4-bar mechanism with only one actuator produces a definite motion with a definite trajectory, however, adding another link and another actuator to the 4-bar mechanism, a 2-RRR PPM is produced which generate a definite motion but with many trajectories. Adding another arm (2-link with one actuator) to the 2-RRR PPM, a 3-RRR PPM will be produced and the generated workspace

has been reduced to the half. However this disadvantage of the workspace, inside the workspace the 3-RRR PPM gives a high performance to do tasks and it will be shown in this work.

2.2 2-RRR Non-Redundant PPM

In Fig. 1 represents the configuration of 2-RRR PPM which is consisted of the two arms. Each arm is consisted of one active joint A_i where $i=1, 2$ for arms 1, 2 respectively, one passive joint B_i , one active link r_i , which connects the active joint A_i to the passive joint B_i and one passive link l_i , which connects the passive joint B_i to the EE.

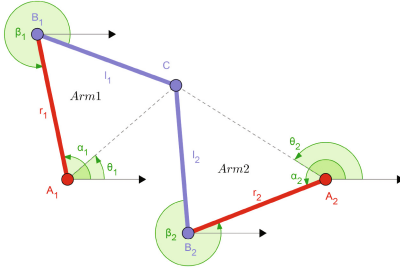


Fig. 1. The 2-RRR PPM.

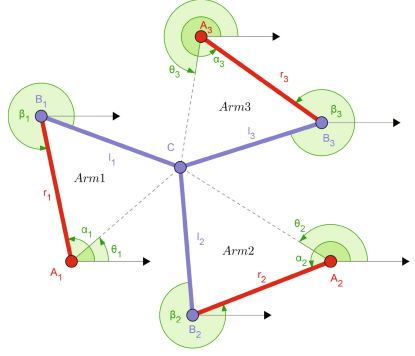


Fig. 2. The 3-RRR PPM.

2.3 3-RRR Redundant PPM

One can see that from the Fig. 2, the 3-RRR PPM mechanism is consisted of the 3 arms. Each arm is consisted of one active joint A_i where $i=1, 2, 3$ for arms 1, 2, 3 respectively. One passive joint B_i , one active link r_i - which connects the active joint A_i to the passive joint B_i . One passive link l_i - which connects the passive joint B_i to the EE. The three active joints A_i are located at the apex of an equilateral triangle, and the end of the three arms are connected together at point to produce the EE of our mechanism.

3 Kinematic Model

3.1 Forward Kinematic Model (FKM)

3.1.1 2-RRR Non-Redundant PPM

From Fig. 1, the independent equations of this system can be derived to describe the boundaries of the workspace. The two circular loci of EE are:

$$(C_x - b_{1x})^2 + (C_y - b_{1y})^2 = l_1^2 \quad (1)$$

$$(C_x - b_{2x})^2 + (C_y - b_{2y})^2 = l_2^2 \quad (2)$$

$$\begin{bmatrix} G_1 & G_2 \end{bmatrix} \begin{bmatrix} C_x \\ C_y \end{bmatrix} = [l_2^2 - l_1^2 - G_3] \quad (3)$$

where:-

$$G_1 = 2b_{1x} - 2b_{2x}$$

$$G_2 = 2b_{1y} - 2b_{2y}$$

$$G_3 = (b_{2x}^2 + b_{2y}^2) - (b_{1x}^2 + b_{1y}^2)$$

3.1.2 3-RRR Redundant PPM

From Fig. 2, the three independent equations of this system can be derived to describe the boundaries of the workspace. The three circular loci of EE (point C) are:

$$(C_x - b_{1x})^2 + (C_y - b_{1y})^2 = l_1^2 \quad (4)$$

$$(C_x - b_{2x})^2 + (C_y - b_{2y})^2 = l_2^2 \quad (5)$$

$$(C_x - b_{3x})^2 + (C_y - b_{3y})^2 = l_3^2 \quad (6)$$

Subtracting Eq. (4) from Eq. (5) and Eq. (4) from Eq. (6), one can obtain that:

$$G_1 C_x + G_2 C_y + G_3 = l_2^2 - l_1^2 \quad (7)$$

$$G_4 C_x + G_5 C_y + G_6 = l_3^2 - l_1^2 \quad (8)$$

Rearranging Eqs. (7) and (8) as a matrix equation form:

$$\begin{bmatrix} C_x \\ C_y \end{bmatrix} = \begin{bmatrix} G_1 & G_2 \\ G_4 & G_5 \end{bmatrix}^{-1} \begin{bmatrix} l_2^2 - l_1^2 - G_3 \\ l_3^2 - l_1^2 - G_6 \end{bmatrix} \quad (9)$$

where:

$$G_1 = 2b_{1x} - 2b_{2x}$$

$$G_2 = 2b_{1y} - 2b_{2y}$$

$$G_3 = (b_{2x}^2 + b_{2y}^2) - (b_{1x}^2 + b_{1y}^2)$$

$$G_4 = 2b_{1x} - 2b_{3x}$$

$$G_5 = 2b_{1y} - 2b_{3y}$$

$$G_6 = (b_{3x}^2 + b_{3y}^2) - (b_{1x}^2 + b_{1y}^2)$$

For 3-RRR PPM with actuation on the first joint, the polynomial solution to the **Direct Kinematics** problem is obtained by setting

$$[b_{ix}b_{iy}]^T = [a_{ix} + r_i C\alpha_i a_{iy} + r_i S\alpha_i]^T$$

where:-

$$C\alpha_i = \cos(\alpha_i), S\alpha_i = \sin(\alpha_i)$$

3.2 Inverse Kinematic Model (IKM)

In triangle A_1B_1C shown in Fig. 2, a relation between the angle α_1 and the point C can be found, and using the **Law of Cosines**:

$$(B_1C)^2 = (A_1B_1)^2 + (A_1C)^2 - 2(A_1B_1)(A_1C)\cos(\alpha_1 - \theta_1)$$

the angle α_1 can be obtained as follow:

$$\alpha_1 = \arccos\left(\frac{(A_1B_1)^2 + (A_1C)^2 - (B_1C)^2}{2(A_1B_1)(A_1C)}\right) + \theta_1 \quad (10)$$

and for θ_1 we find that

$$\theta_1 = \arctan \frac{C_y - a_{1y}}{C_x - a_{1x}} \quad (11)$$

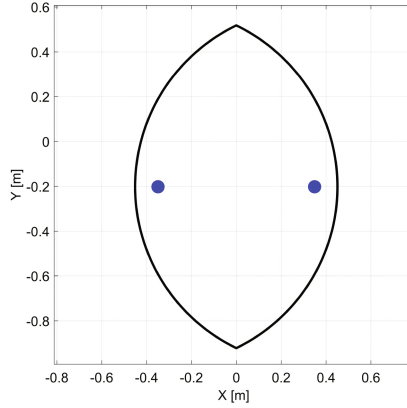
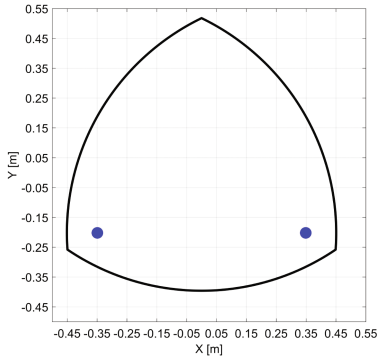
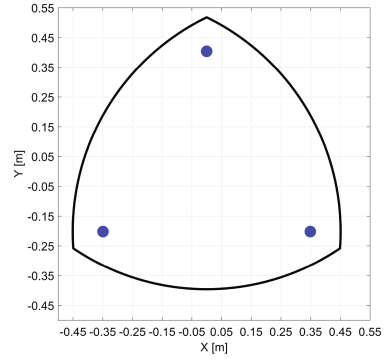
Notice that, $A_1B_1 = r_1$, $B_1C = l_1$ and it is easy to determine A_1C and it will be as follow:-

$$A_1C = \sqrt{(C_y - a_{1y})^2 + (C_x - a_{1x})^2} \quad (12)$$

The similar derivation can also be used for determining α_2 and α_3 .

4 Workspace Analysis

The *workspace* (WS) for the presented PPM is the area where the EE can move through. To determine this area, there are two constraints that create the circles around the active joint a_i , the radius of first one is $|r_i + l_i|$ while the other is $|r_i - l_i|$. Each circle centered at a_i where $i = 1, 2, 3$ for 3-RRR PPM and $i = 1, 2$ for the 2-RRR PPM. The intersection of two circles construct the whole workspace for the 2-RRR PPM as shown in Fig. 3, however the interested area are the upper one as in Fig. 4. The intersection of three circles produce the workspace for the 3-RRR as shown in Fig. 5. For the 2-RRR PPM have a divided WS, upper and lower. The research in operating the 2-RRR PPM shows that the operation can be done in one part and moving to the other one need a control trick and a mechanical combination to allow working in both area [10]. When comparing these figures, note that, Figs. 4 and 5 are double scale of Fig. 3.

**Fig. 3.** WS for whole 2-RRR PPM**Fig. 4.** WS for 2-RRR PPM**Fig. 5.** WS for The 3-RRR PPM

5 Jacobian Matrix

Another types of research is the PM performance. An important question that arises in the process of designing robotic manipulators is the choice of optimization and performance criteria. In the context of kinematics, several concepts have been used as design guidelines. Some authors develop some definitions that help in optimization and improving the performance of **PPM** such as *manipulability* and *dexterity* indices within the workspace. Differentiating Eq. (9) with respect to time to generate a relationship between joint rates and EE velocities and with some mathematics, one can found:

$$J_x \dot{x} = J_q \dot{q} \quad (13)$$

where $J_x = \frac{\partial f}{\partial x}$ and $J_q = \frac{\partial f}{\partial q}$ Thus, the Jacobian equation can be written in the form:

$$\dot{q} = J \dot{x} \quad (14)$$

where $J = J_q^{-1}J_x$, if the manipulator is non-redundant, i.e., number of actuators is equal to DOF, then: $\dot{x} = J^{-1}\dot{q}$. In redundant mechanism, the number of actuators is greater than the DOF, therefore: $\dot{x} = J^+\dot{q}$. The vector loop of each arm can be found as:

$$C_x = x_{ai} + r_i \cos(\alpha_i) + l_i \cos(\beta_i) \quad (15)$$

$$C_y = y_{ai} + r_i \sin(\alpha_i) + l_i \sin(\beta_i) \quad (16)$$

The manipulator's jacobian matrix is presented, so, by differentiating Eqs.(15) and (16):

$$\dot{C}_x = -r_i \sin(\alpha_i)(\dot{\alpha}_i) - l_i \sin(\beta_i)(\dot{\beta}_i) \quad (17)$$

$$\dot{C}_y = r_i \cos(\alpha_i)(\dot{\alpha}_i) + l_i \cos(\beta_i)(\dot{\beta}_i) \quad (18)$$

Solving Eqs. (17) and (18) which can be done by multiplying Eq. (17) with $\cos(\alpha_i + \beta_i)$ and Eq. (18) with $\sin(\alpha_i + \beta_i)$, this will be as following:

$$\cos(\beta_i)\dot{C}_x = -r_i \sin(\alpha_i) \cos(\beta_i)(\dot{\alpha}_i) - l_i \sin(\beta_i) \cos(\beta_i)(\dot{\beta}_i)$$

$$\sin(\beta_i)\dot{C}_y = r_i \cos(\alpha_i) \sin(\beta_i)(\dot{\alpha}_i) + l_i \sin(\beta_i) \cos(\beta_i)(\dot{\beta}_i)$$

and adding these two previous equations:

$$\cos(\beta_i)\dot{C}_x + \sin(\beta_i)\dot{C}_y = -r_i \sin(\alpha_i) \cos(\beta_i)(\dot{\alpha}_i) + r_i \cos(\alpha_i) \sin(\beta_i)(\dot{\alpha}_i) \quad (19)$$

using the trigonometry equations the final result will be:

$$\cos(\beta_i)\dot{C}_x + \sin(\beta_i)\dot{C}_y = r_i \sin(\beta_i - \alpha_i)\dot{\alpha}_i \quad (20)$$

Then Eq. (20) is as the form of Eq. (13), and by expanding Eq. (20), the result for 3-RRR PPM is:

$$J_x = \begin{bmatrix} \cos(\beta_1) \sin(\beta_1) \\ \cos(\beta_2) \sin(\beta_2) \\ \cos(\beta_3) \sin(\beta_3) \end{bmatrix}$$

$$J_q = \begin{bmatrix} r_1 \sin(\beta_1 - \alpha_1) & 0 & 0 \\ 0 & r_2 \sin(\beta_2 - \alpha_2) & 0 \\ 0 & 0 & r_2 \sin(\beta_3 - \alpha_3) \end{bmatrix}$$

and for the 2-RRR PPM is:

$$J_x = \begin{bmatrix} \cos(\beta_1) \sin(\beta_1) \\ \cos(\beta_2) \sin(\beta_2) \end{bmatrix}$$

$$J_q = \begin{bmatrix} r_1 \sin(\beta_1 - \alpha_1) & 0 \\ 0 & r_2 \sin(\beta_2 - \alpha_2) \end{bmatrix}$$

6 Singularity Analysis

Considering Eq. 13, three types of singularities can be defined for parallel manipulators [17]:

1. Direct kinematic singularities when J_x is singular.
2. Inverse kinematic singularities when J_q is singular.
3. Combined (complex) singularities when J_x and J_q are singular.

Direct singularities (*i.e.*, $|J_x| = 0$) take place when there are some nonzero velocities of the end-effector that are possible with zero velocities at the actuators. Also, direct kinematic singularities are referred to as force uncertainties or as force unconstrained poses. On the other hand, inverse singularities (*i.e.*, *when* $|J_q| = 0$) happen when there exist some nonzero actuator velocities that cause zero velocities for the end-effector.

7 Dexterity Index

Dexterity index (DI) is a measure of a manipulator to achieve different positions and orientations for each point within the workspace. DI shows the various properties of a manipulator. It illustrates the singularity points and also gives an indication for the nearest singular configuration. Therefore, the use of condition number is an indication of the amplification of the error on the position of EE. This number is to be kept as small as possible. The condition number can be found by Singular Value Decomposition SVD of the Jacobian matrix because our manipulator is redundant:

$$J = U\Sigma V^T \quad (21)$$

where $J = J_q^{-1}J_x$. The condition number is defined as the ratio of the largest singular value, σ_{max} , to the smallest one, σ_{min} and therefore, $k = \sigma_{max}/\sigma_{min}$ which represents the amount of change in the EE for one unit of change of the actuators. Using the reciprocal of k -helps to be presentable- and called it η which is the *dexterity index* and it will change from 0 to 1. Trying to approach a condition number close to one helps the manipulator to have an accuracy close to the accuracy of the actuators and to maintain a good stiffness which are desirable characteristics. $\eta = \sigma_{min}/\sigma_{max}$ Applying these previous equations for each point in the whole workspace, the DI map for 2-RRR PPM and 3-RRR PPM are shown in Figs. 6 and 7 respectively. From Fig. 6 for the 2-RRR PPM it is found that the maximum values of DI located at top left, where these points give a best dexterity performance for the 2-RRR PPM. The minimum values of DI are distributed at very large area in the workspace such as at the boundaries of the workspace and also between the active joints locations, which give a poor performance to the manipulator. In Fig. 7, it is obvious that the maximum DI values are located at the center of the workspace where a good performance has been occurred, however, the minimum values are located around the active joints location of

3-RRR PPM, which have a poor performance. It is found that from the figures below, the DI map for 2-RRR PPM is smaller and approach to zero at some points and others closed to one, but it is not symmetrical, however, for the 3-RRR PPM it found that the DI map is distributed symmetrically. Consequently, the 3-RRR PPM have a good characteristics than the 2-RRR PPM. When comparing this DI values for 2-RRR PPM and 3-RRR PPM respectively, it is found that - for example - the area surrounding by 0.4 contour is at the upper left side for 2-RRR PPM and around the center for 3-RRR PPM. Over that, in 3-RRR PPM, this area is larger than in 2-RRR PPM which it is a very important advantage.

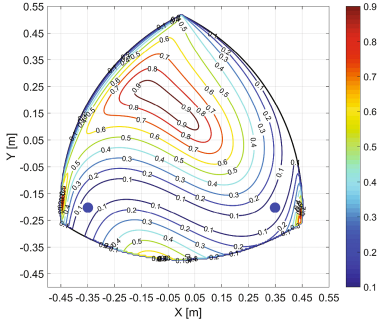


Fig. 6. DI for the 2-RRR PPM.

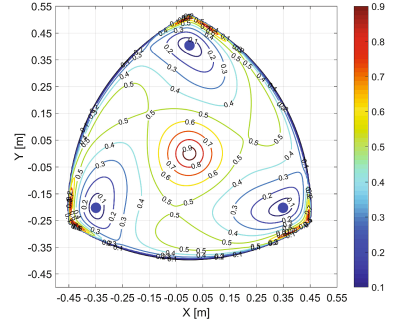


Fig. 7. DI for the 3-RRR PPM.

8 Manipulability Index

Another index that be used to show the performance for the manipulators is the Manipulability Index (MI). MI is the agility to perform a task in a specific workspace [18]. In [19], it is measured as the product of ellipsoid's axes or to be specific is the product of the singular value of the *Jacobian Matrix*:

$$\mu = \sqrt{\det(JJ^T)} = \sqrt{\lambda_1 \lambda_2 \dots \lambda_m} = \sigma_1 \sigma_2 \dots \sigma_m \quad (22)$$

where $\lambda_1, \lambda_2, \dots, \lambda_m$ are the eigenvalues of JJ^T and the $\sigma_1, \sigma_2, \dots, \sigma_m$ are the singular values of J . By applying the previous equations for each point in the whole workspace, the manipulability map for both 2-RRR PPM and 3-RRR PPM are shown in Figs. 8 and 9 respectively. It is found that for the 2-RRR that the maximum value of MI is about 0.35 and located at the top left of the workspace, however, in 3-RRR it is found that the values of MI is up to 0.8 and it is located at the center of the workspace. The manipulability gives that how is the closeness of the accuracy in the velocity between the end-effector and the joints.

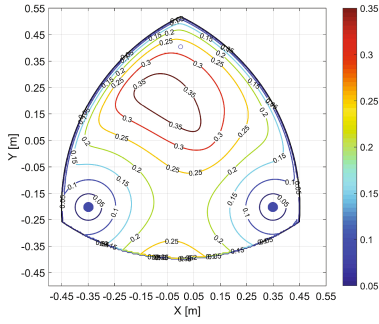


Fig. 8. MI for the 2-RRR PPM.

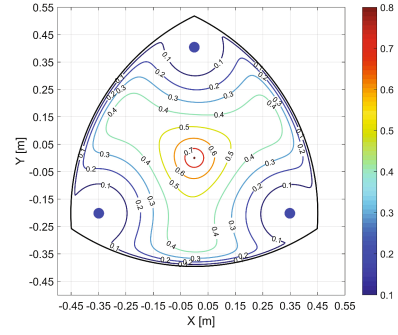


Fig. 9. MI for the 3-RRR PPM.

9 Conclusion

A comparison between 2-RRR PPM and 3-RRR PPM has been done through this research work. The mechanical structure and motion mechanics was investigated for these two PPMs. The workspace and its usability are studied. This is done by passing through the forward and inverse kinematics with the Jacobian matrix. Two performance indices are obtained for this two manipulators; dexterity and manipulability. The simulation work determines and indicates the parameters of these two manipulators. It is found that, the 3-RRR PPM has performance indices better than that of 2-RRR PPM. According to this work, the best parameters and performance indices can be deduced for target of the best values that carried out for a PPM uses. For the Future work, the 3-RRR PPM will be constructed. It is necessary to built this manipulator and applying a specific control algorithm to see how it works. Also, showing the system performance according to the previous deduced indices.

References

1. Patel, Y.D., George, P.M.: Parallel manipulators applicationsa survey. *Mod. Mech. Eng.* **2**(03), 57 (2012)
2. Pandilov, Z., Dukovski, V.: Comparison of the characteristics between serial and parallel robots. *Acta Technica Corviniensis-Bull. Eng.* **7**(1) (2014)
3. Blan, R., Mties, V., Stan, S., Lpuan, C.: On the Control of a 3-RRR Planar Parallel Minirobot. *Mecatronica* (4) (2004)
4. Tsai, L.W.: *Robot Analysis: The Mechanics of Serial and Parallel Manipulators*. Wiley (1999)
5. Dash, A.K., Chen, I.M., Yeo, S.H., Yang, G.: Task-oriented configuration design for reconfigurable parallel manipulator systems. *Int. J. Comput. Integr. Manuf.* **18**(7), 615–634 (2005)
6. Maciejewski, A.A., Klein, C.A.: Obstacle avoidance for kinematically redundant manipulators in dynamically varying environments. *Int. J. Robot. Res.* **4**(3), 109–117 (1985)

7. Nakamura, Y., Hanafusa, H., Yoshikawa, T.: Task-priority based redundancy control of robot manipulators. *Int. J. Robot. Res.* (1987)
8. Wang, J., Gosselin, C.M.: Kinematic analysis and design of kinematically redundant parallel mechanisms. *Trans.-Am. Soc. Mech. Eng. J., Mech. Des.* **126**(1) (2004)
9. Shang, W., Cong, S.: Dexterity and adaptive control of planar parallel manipulators with and without redundant actuation. *J. Comput. Nonlinear Dyn.* **10**(1), 011002 (2015)
10. <http://www.mecademic.com/DexTAR.html>
11. Cheng, H., Yiu, Y.K., Li, Z.: Dynamics and control of redundantly actuated parallel manipulators. *IEEE/ASME Trans. Mechatron.* **8**(4) (2003)
12. Shayya, S., Krut, S., Baradat, C., Pierrot, F.: Dynamic analysis of 4 degrees of freedom redundant parallel manipulator. In: *Advances in Robot Kinematics*, pp. 545–553. Springer (2014)
13. Shang, W., Cong, S., Kong, F.: Identification of dynamic and friction parameters of a parallel manipulator with actuation redundancy. *Mechatronics* **20**(2) (2010)
14. Paccot, F., Andreff, N., Martinet, P.: A review on the dynamic control of parallel kinematic machines: theory and experiments. *Int. J. Robot. Res.* **28**(3), 395–416 (2009)
15. Ghorbel, F.H., Chtelat, O., Gunawardana, R., Longchamp, R.: Modeling and set point control of closed-chain mechanisms: theory and experiment. *IEEE Trans. Control Syst. Technol.* **8**(5), 801–815 (2000)
16. Shang, W.W., Cong, S., Li, Z.X., Jiang, S.L.: Augmented nonlinear PD controller for a redundantly actuated parallel manipulator. *Adv. Robot.* (2009)
17. Gosselin, C., Angeles, J.: Singularity analysis of closed-loop kinematic chains. *IEEE Trans. Robot. Autom.* **6**(3), 281–290 (1990)
18. Yoshikawa, T.: Manipulability of robotic mechanisms. *Int. J. Robot. Res.* **4**(2), 3–9 (1985)
19. Zhang, P., Yao, Z., Du, Z.: Global performance index system for kinematic optimization of robotic mechanism. Contributed by the Mechanisms and Robotics Committee of ASME for Publication in the *Journal of Mechanical Design*

Proceedings of the International Conference on
Advanced Intelligent Systems and Informatics 2017
Hassanien, A.E.; Shaalan, K.; M. Gaber, T.; Tolba, F.M.
(Eds.)
2018, XX, 917 p. 433 illus., Softcover
ISBN: 978-3-319-64860-6